Ferromagnetic/Superconducting All Oxide Superlattices and Heterostructures

H.-U Habermeier [*] ***and G. Cristiani***

Max-Planck-Institut für Festkörperforschung, Stuttgart, Germany

The physical properties of the perovskite-type oxide $RuSr_2GdCu_2O_8$ have been recently discussed in the view of a simultaneous occurrence of superconductivity and ferromagnetism. In order to explore some peculiarities of these compounds we have prepared superlattices of oxides that are known to be either ferromagnetic ($La_{.67}Ca_{.33}MnO_3$) or superconducting ($YBa_2Cu_3O_7$). These superlattices serve as model systems to understanding the physics of $RuSr_2GdCu_2O_8$. The YBCO/LCMO superlattices have been grown by pulsed laser deposition with individual layer thickness ranging from 4 to 200 unit cells for the $YBa_2Cu_3O_7$ and 10 to 500 unit cells for the $La_{.67}Ca_{.33}MnO_3$. Measuring dc-transport and magnetic properties some novel effects have been found due to a coupling between the layers observed in the superlattices. Superlattices with individual thickness of the constituent materials of 4 nm e.g. show a reduced Curie temperature of 120K and a superconducting transition temperature of 52K. Lowering the temperature of reentrant normal state occurs at T = 25K. Switching off the electronic interlayer coupling by the introduction of insulating $SrTiO_3$ spacer layers leads to the intrinsic critical temperatures. For the explanation of the results several novel concepts have to be developed based on a long range ferromagnetic interlayer coupling and a novel long range superconducting proximity effect.

1. Introduction:

Ferromagnetism (FM) and superconductivity (SC) are antagonistic by nature. Superconductivity is manifested by the formation of Cooper pairs, where charge carriers with antiparallel spinorientation are coupled, e.g., by elementary excitations such as phonons. The existence of a spontaneous magnetization in a ferromagnet, on the other hand, arises from the surplus of charge carriers with one spin orientation, consequently, both ordering mechanisms rule out each other. Additionally, in conventional s-wave

[*] E-mail: huh@servix.mpi-stuttgart.mpg.de

superconductors local magnetic moments break the spin singlet Cooper pairs and, thus, strongly suppress superconductivity. Therefore, uniform FM and SC can not coexist. Similarly, injection of spinpolarised quasiparticles into superconductors result in a suppression of superconductivity due to the breaking of time-reversal symmetry of the Cooper pairs. There are, however, several intermetallic compounds where SC occurs in the presence of coupled magnetic ions occupying all one specific crystallographic site [1]. All these intermateallic compounds have in common that the superconducting ordering temperature, T_c, is substantially higher compared to the Néel temperature, T_N, or the Curie temperature, Θ_c, respectively [2]. The parent compound for the high temperature superconductors (HTS) such as La_2CuO_4 is an antiferromagnetic (AFM) insulator and SC upon doping with holes is regarded as being mediated by antiferromagnetic fluctuations of the Cu spins. The existence of an AFM ground state is seen as a necessary prerequiste for the occurrence of SC in the cuprates. Many of these materials contain magnetic ions isolated from the conducting CuO_2 planes. In all these cases T_N is quite low; for the $Rba_2Cu_3O7_{-X}$ system, e.g., with R= Gd, T_C = 92K and T_N = 2K only.

The motivation to study the interrelation of superconductivity and ferromagnetism in oxide system arises from the fundamental interest of the common aspects and potential differences of the pyhysical properties of artificially layered metallic FM/SC and oxide systems. Thus, it includes dimensionality effects and the possibility of an oscillatory behavior of T_C as a function of the FM layer thickness which has been discussed in terms of a periodic "π" phase switching. Here, the order parameter changes sign under the transition through FM layers. An analogy can be seen in the metallic GMR materials where FM films are sandwiched in between normal metal films and couple either ferro- or antiferromagnetic, depending on the normal metal thickness. Aspets of the different pairing symmetry of conventional SC's and HTS materials will be accounted for these differences. Secondly, the possibility to investigate spin-polarized quasiparticle injection into cuprate superconductors and its effects on superconductivity is an interesting field for fundamental physics with potential applications in spin electronics. A third reason arises from some controversially discussed properties of the (ferro) magnetic superconductor $RuSr_2GdCu_2O_8$ with a charge reservoir block containing magnetically ordered Ru^{5+} spins intercalated by the CuO_2 -Gd-CuO_2 layers which are believed to cause SC [3 - 5]. This compound undergoes a magnetic transition at 130 – 140K followed by a superconducting transition at 20K – 50K. the interplay of magnetic and superconducting properties of these compounds is a topic of current concern.

Due to the layered nature of the $RuSr_2GdCu_2O_8$ compound this material can be regarded as an intrinsic superlattice (SL) and its properties can be mimicked by SL's consisting of individual superconducting and ferromagnetic

layers. Modifications of the modulation length of the SC and FM layers, respectively, are an experimental tool to tailor the coupling between the ferromagnetic and superconducting layers in a stack. Additionally, introuducing insulating spacers in between the SC and FM layers and/or pairs of SC/FM sandwiches opens possibilities for the investigation of interface and tunneling phenomena. Earlier work with metallic s-wave SC's and ferromagnetic metals demonstrates that thin SC films sandwiched in between FM metal films have a strongly reduced T_C compared to isolated ones [6]. This paper deals with SL's with oxide ferromagnets such as the doped La-manganites and the oxide SC $Yba_2Cu_3O_{7-x}$ (YBCO). Both have a highly anisotropic Fermi surface and the SC part is regarded as anisotropic d-wave. The advantages of the combination superate/ manganite SL's is seen in their all oxide nature, crystal structure compatibility and partially adjustable lattice parameters of La-manganite part. The electronic structure of the manganites is determined by lifting of the degeneracy of the Mn^{3+} 3d electrons due to the crystal field of the surrounding oxygen octahedral and the Jahn-Teller effect. According to Hund's rules the 3d electrons are oriented with paralledl spin and the e_g band is 100% spin-polarized. Consequently, spin transport and spin injection studies can be performed. This opens a novel access to realize of superconductor 3-terminal devices. Based on earlier studies of cuprate/manganite heterostructures [7 - 9], systematic investigations are presented in this paper modifying the superlattice composition and investigating their impact on the magneti and transport properties.

2. Experimental Details and Results:

Superlattices consisting of m unit cells of $YBa_2Cu_3O_{7-x}$ and n unit cells of $La_{2/3}$ $Ca_{1/3}$ MnO_3 (LCMO) repeated N times – $(m,n)_N$ SL's – and thus of different modulation lengths, Λ, have been deposited at 730^o C at an oxygen pressure of 5.10^{-3} Pa by pulsed laser deposition technique [10, 11] onto $SrTiO_3$ single crystal substrates and *in-situ* annealed in 1 atm oxygen for 1 hour at 530^{o}C. The deposition system (high vacuum chamber in conjunction with a KrF Excimer laser) is equipped with FIR pyrometric temperature control of the radiatively heated substrate and growing film to ensure a constant temperature at the groth front. Figure (1) represents a schematic drawing of the apparatus. A computer controlled target exchange system accommodating up to 5 different targets facilitates the desired SL formation. Thickness control of the individual layers is done by pulse counting after some calibration runs to ensure the stability of the ratio film thickness per pulse. Details of the deposition system optimized for SL preparation will be published elsewhere [12]. The composition of the superlattices is characterized either by the indvidual layer thickness t_{YBCO} and t_{LCMO} for the YBCO and LCMO layers, respectively, and the number of layers N or by the number of unit cells and $(m, n)_N$. In Table (1), the

composition of the SL's investigated are listed together with the measured data for T_c and Θ_c. The X-ray diffraction pattern confirms phase purity of the c-axis oriented films (c.f. Fig.2) and shows peaks with a rather large FWHM of 2^o – 4^o. Superlattice peaks as expected due to the additional scattering planes in a superlattice are barely to be identified. A determination of the SL peak positions according to the standard formula $\Lambda = \lambda/2\ (\sin\Theta_n - \sin\Theta_{n+1})^{-1}$ shows that for the first and second order peaks for our SL with the smallest modulation length Λ = 13 nm the peak positions to be expected are buried in the main peak. A deconvolution of the diffraction peaks and a modeling using the SUPREX program [13] is underway.

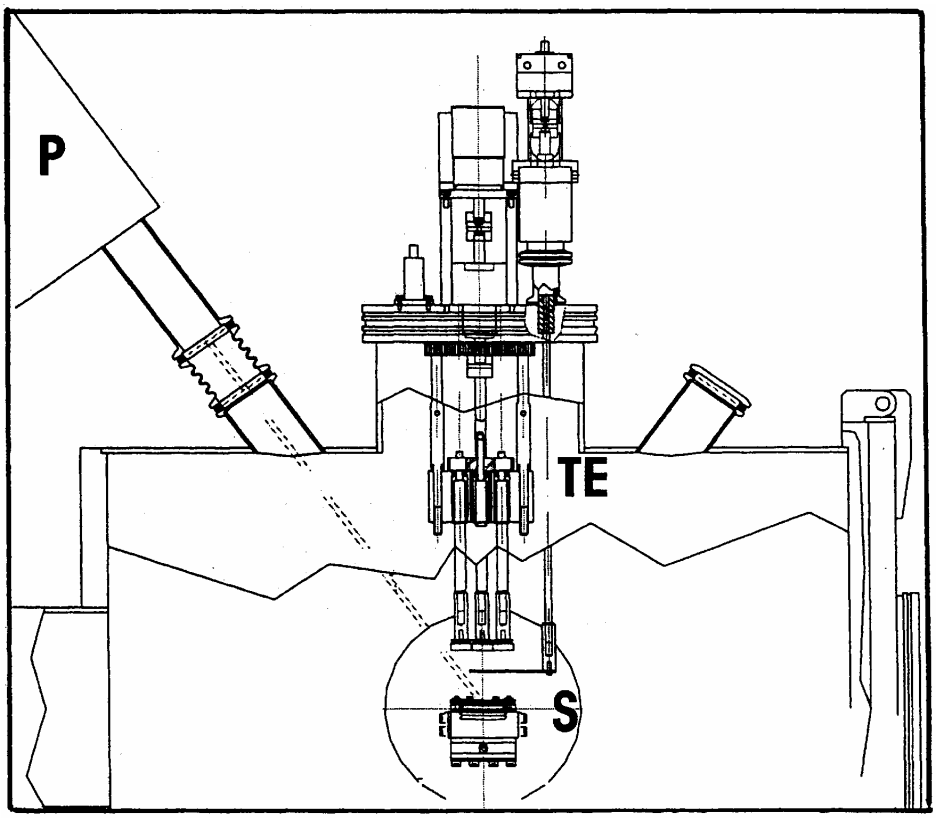

Fig. (1): Schematic drawing of the deposition chamber with target exchanger [TE], Pyrometer [P] and substrate heater [S].

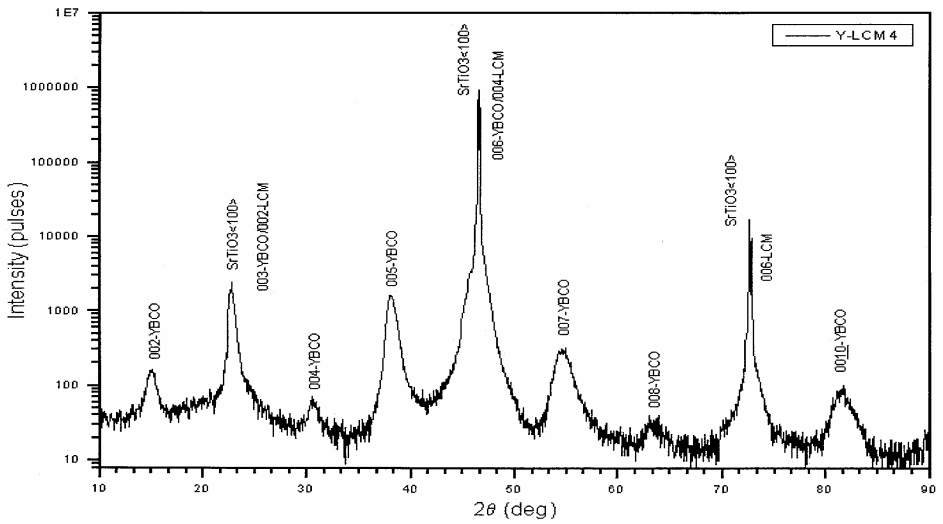

Fig. (2): X-ray diffraction pattern of a (7.5 nm/ 5nm)$_{20}$ YBCO/LCMO superlattice.

Table. (1): Composition of the superlattices investigated and corresponding critical temperatures for the ferromagnetic (Θ_C) and superconducting (T_C) transition.

Sample	t_{YBCO} (nm)	t_{LCMO} (nm)	t_{STO} (nm)	N	Θ_C (K)	T_C (K)
1	50	50	0	1	240	68
2	20	20	0	5	153	50
3	20	40	0	5	150	20
4	20	80	0	5	215	< 4.2
5	40	20	0	5	150	70
6	80	20	0	5	150	86
7	7.5	5	0	20	115	52
8	100	100	10-isolating pairs	5	245	82
9	100	100	10	5	250	87

Representative cross-sectional TEM micrographs are given in Fig. (3a and b) for low and high resolution. In the low magnification image (Fig. 3a) the interfaces appear to be somewhat wavy. A similar waviness is commonly observed in SL'S containing YBCO and is not likely related to strain relaxation. The high-resolution image along a perovskite cube direction (Fig. 3b) show that the interfaces are atomically flat. The expitaxial relationship is clearly "cube-on-cube". This is confirmed by electron diffraction (insert of Fig. 3a) taken over film and substrate. The LCMO bands are easily identified as the darker regions in Fig. (3a) and no interconnections between LCMO layers are present.

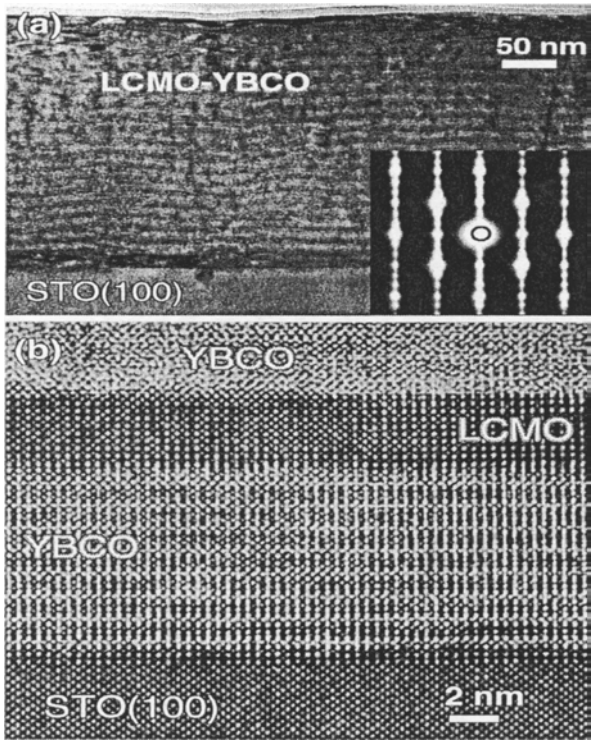

Fig. (3): (a) Low resolution cross-sectional TEM and diffraction pattern of a $(7.5nm/5nm)_{20}$ YBCO/LCOM superlattice; (b) corresponding high resolution cross-sectional TEM.

The magnetic moments of the films are determined using standard SQUID magnetometry; the transport properties are measured by 4-point probe techniques using evaporated gold contacts and a probing current of 0.1mA. In Fig. (4) the R(T) and M(T) curves of a 50 nm YBCO/50 nm LCMO heterostructure is represented, indicating clearly the Curie temperature of the LCMO of 250K and the superconducting transition at 70K. Whereas Θ_c is slightly reduced as compared to the bulk value of 275K and corresponds well to that strain lean films of comparable thickness [14], T_C is reduced by approximately 20K and thus much smaller than T_C=89-90 K of isolated YBCO films of comparable thickness. This heterostructure demonstrates that the individual properties – FM and SC – of the constituents have been preserved, some mutual influence of SC and FM, however, seems to be present. In order to systematically change this interaction, we prepared SL's of different compositions of the $[t_{YBCO}/t_{LCMO}]_N$- type, keeping either t_{YBCO} constant and change t_{LCMO} or vice versa. Figure (5) represents the R (T) and M (T) plots of the film #5 with T_C= 70K and Θ_C = 150K. The normal state properties are expected to be a superposition of the linear dependence R~T of the YBCO and the features of the metal-insulator transition of the LCMO. The metal-insulator transition appears as a change in the slope of the R (T) around Θ_C. SL's with t_{YBCO} = 20 nm

and t_{LCMO} = 20. 40 and 80 nm show a systematic nonlinear decrease of T_C. SL's of this series with t_{LCMO} = 80 nm show no superconductivity above 4.2 K (c.f. Fig. 6). On the contrary, keeping t_{LCMO} = 20 nm and increasing the thickness of the YBCO layer in the SL causes a systematic increase of T_C up to 86K (c.f. Tab I). The ferromagnetic ordering temperature in all these films – with the exception of the LCMO dominated film # 4 - is around 150K. SL's with much thinner individual layers such as sample # 7 ($(7.5/5)_{20}$) show a quite different behavior. Θ_C is reduced to 115K and T_C is 52K; at lower temperatures, however, a reentrant normal state appears. The onset of the reentrant normal state (30K) is at the same temperature where the approach to saturation of the magnetic moment occurs (c.f. Fig. 7).

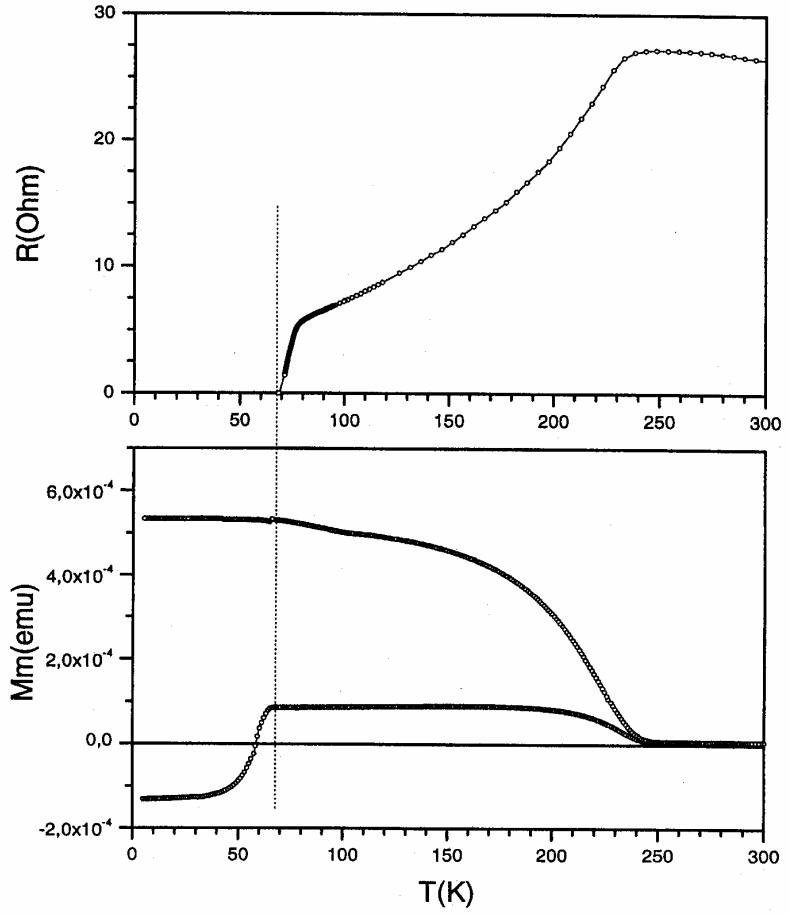

Fig. (4): Resistance (upper panel) and magnetic moment (lower panel) of a 50nm YBCO/50nm LCMO hetersostructure as a function of temperature. The ZFC measurement shows a diamagnetic signal.

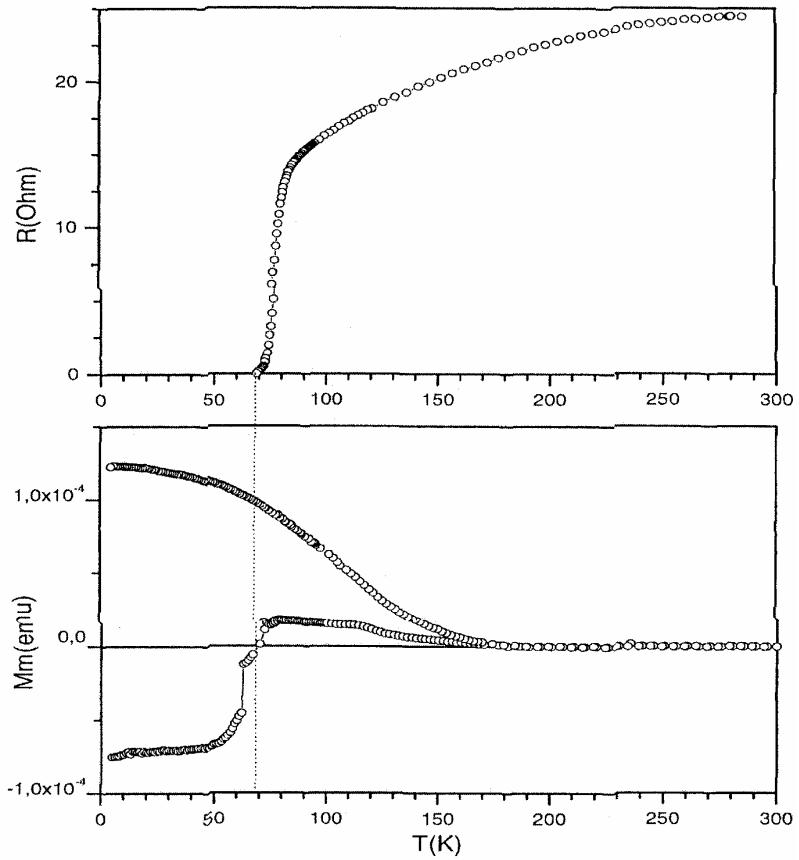

Fig. (5): Resistance (upper panel) and magnetic moment (lower panel) of a (40 nm YBCO/ 20nm LCMO)$_5$ superlattice as a function of temperature. The ZFC measurement shows a diamagnetic signal.

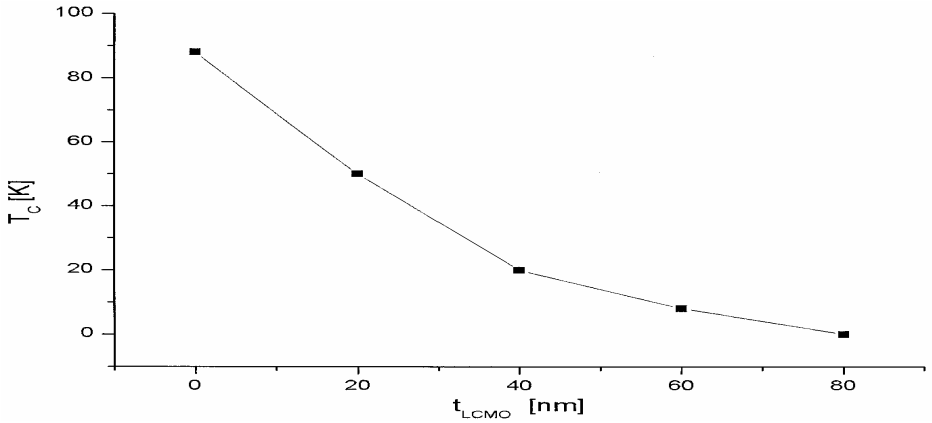

Fig. (6): T_C reduction as a function of LCMO layer thickness in YBCO/LCMO superlattices.

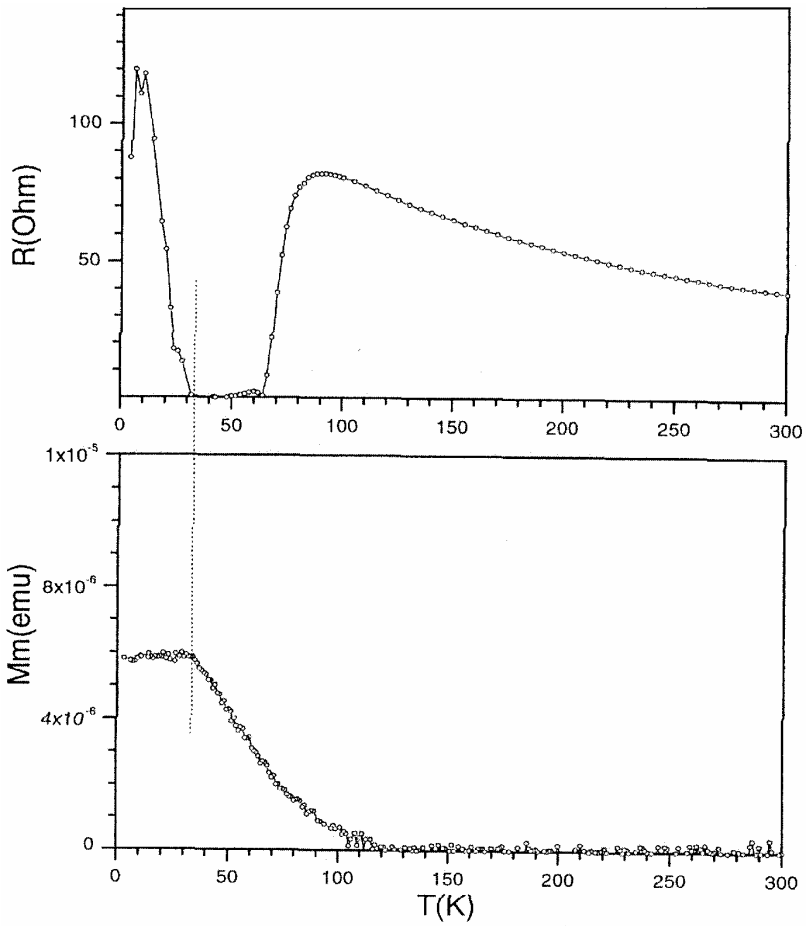

Fig. (7): Resistance (upper panel) and magnetic moment (lower panel) of a (7.5 nm YBCO/ 5 nm $LCMO)_{20}$ superlattice as a function of temperature indicating the reentrant normal state at 30 K.

Investigation of the magnetic flux penetration using the magneto-optical Faraday-effect revealed only for the YBCO dominated SL # 6 the flux penetration profiles typical for YBCO thin films [15], in all the other SL's investigated, no phase boundary between the Shubnikov phase and the Meissner phase could be observed. This behaviour is typical for materials with homogeneous flux distribution. All specimens with the exception of # 6 show no Meissner-effect in the magnetization measurements. This is indicative for the spontaneous vortex state as discussed by Chu [16] for the $RuSr_2GdCu_2O_8$ and related compounds.

3. Discussion:

The reduction of Θ_C in the SL's from the bulk value of ~275K has been observed by other authors [8] and only discussed in the literature so far by Habermeier et al. [17]. The reasons for this reduction are not yet clear. Problems with oxygen stoichiometry could be accounted for, but neither careful post deposition plasma-oxidation nor annealing in 1 atm oxygen in a temperature range, where the microstructure is not affected, indicated changes of Θ_C. Charge transfer between YBCO and LCMO, which has been discussed in the case of YBCO/ PrBCO SL's, would modify the hole concerntraion of the LCMO layers and, thus, change the Curie temperature. According to the phase diagram of the La-Ca-Mn-O system [20], however, no ferromagnetic metallic state can be expected with Θ_C lower than 190K and a considerable charge transfer would lead to an insulting charge ordered state. The data given in Table. (1) show, that the observed values for Θ_C are much lower than the minimum Θ_C according to the phase diagram. Strain effects cannot completely be ruled out. The cubic lattice parameter of the $La_{2/3}Ca_{1/3}MnO_3$ is 0.386 nm, i.e., close vicinity to the average lattice parameter of twinned YBCO films (< a, b > = 0.358nm). This small epitaxial tensile strain (~ 0.14 %), however, can cause an estimated reduction of Θ_C smaller than 5K [14]. There are several papers dealing with magnetic coupling in ferromagnetic/normal metal multi-layers. The prevailing experimental evidence indicates that the exchange coupling with metal spacers is short range (1-13 nm) and a thickness dependent crossover from FM to AFM coupling occurs. These arguments derived from metallic SL's cannot simply be transferred to oxide SL's. The short-range spin diffusion length of several nanometers in metallic FM systems will confine the interaction effect due to the neighboring metal layer to a region of less than 5 nm close to the interfaces. In the case of the oxide SL's, the interaction length must be apparently long range (10 – 30 nm). The close vicinity of Θ_C with the temperature for the spin gap opening in the YBCO normal state suggests the interrelation of the two temperatures. A reduced ploarizability of the charge carrier spins below the spin gap opening temperature can be the reason for this effect. A certain analogy to the model of Sa de Melo [19] can be seen, which predicts a modification of the density of states and a weakening of the coupling via the appearance of a superconducting gap. Probably the spin gap plays that role in the oxide SL's. This model, however, is based on an RKKY-type indirect exchange coupling between ferromagnetic layers.

The observed reduction of T_C in superlattices is not a new effect and has been studied in detail in the case of non-conducting spacer layers, e.g., $PrBa_2Cu_3O_7$ (PBCO). Several models have been discussed ranging from intercell coupling; Kosterlitz-Thouless transition, long-range proximity effect and charge tranfer between YBCO and PBCO. Jansen and Block [20] give a

review and develop a theoretical model for the direct correlation between T_C (m,n) and the normal state properties based on indirect exchange Cooper pairing between conduction electrons via oxygen anions. Experimentally, Li et al. [21] as well as Lowndes et al. [22] find that with increasing PBCO layers thickness T_C decreases from 93K rather rapidly up to n=4 and then saturates with increasing n. The initial drop is most marked for m=1, leading to a T_C of 30K. For m=1, 2, 3, 4 and 8, T_C for a PBCO thickness of 20 nm (n=16) amounts to 20, 54, 71, 80, and 87K, respectively. In our case, however, the smallest value for m studied so far is m =4 where a T_C of 80K would be expected for the YBCO/PBCO case which is substantially higher than the measured value of 52K in the YBCO/LCMO case. Furthermore, the results given in Fig. (6) for m = 17 and n 72 – 207 unit cells show a drastic drop of T_C with increasing n and vanishing superconductivity for n = 207. these findings are not compatible with the YBCO/PBCO results and indicate that another long-range mechanism has to be accounted for the T_C reduction.

The explanation for the reduction of the ordering temperatures shown so far must be based on the interaction of the electronic systems of the YBCO and LCMO layers. A tentative check of this assumption is seen in the introduction of an insulating spacer layer in between of YBCO and LCMO. This will switch off – or at least reduce – this interaction and, thus, it is expected that the intrinsic behavior of individual layers is restored. In Fig. (8) and Table (1) (sample # 8 and #9) the results for R (T) and M (T) are given for symmetric SL's consisting of (YBCO 100nm/ STO 10nm)$_5$ (#9) and (YBCO 100nm/ LCMO 100nm/Sto 10nm)$_5$ [#8]. Indeed, T_C and Θ_C arerestored close to the original values of the single layers films, thus indicating the role of the interaction of the electronic systems of the individual layers.

The experiments performed so far clearly demonstrate the existence of a novel long-range proximity effect in all-oxide ferromagnetic superconducting superlattices. In order to study further details of this long range proximity effect measurements using far infrared spectroscopic ellipsometry have been performed. They show a strong decrease of the free carrier responses in the normal and superconducting state of YBCO involving and unexpected large length scale in the order of 20nm and 10nm in YBCO and LCMO, respectively [25]. Further experiments are designed to study the SC/FM interaction by replacing LCMO by $SrRuO_3$ which is an intinerant FM system with Θ_C = 160K and not a double-exchange ferromagnet such as LCMO. First experiments show strong similarities with the results presented here such as the reduction of the Curie temperature, T_C and conductivity, however, there are some remarkable differences like the stronger suppression of ferromagnetism in the YBCO/SRO superlattices. Further research will be directed towards to the substitution of LCMO by other oxide conductors, ferromagnetic, antiferromagnetic, or just

metallic. This is intended to affect the spin fluctuations in the cuprates due to the frustration of the nearest-neighbor antiferromagnetic Cu^{2+}-Cu^{3+} correlations which have been suggested to be relevant for the d-wave pairing of the superconducting cuprates.

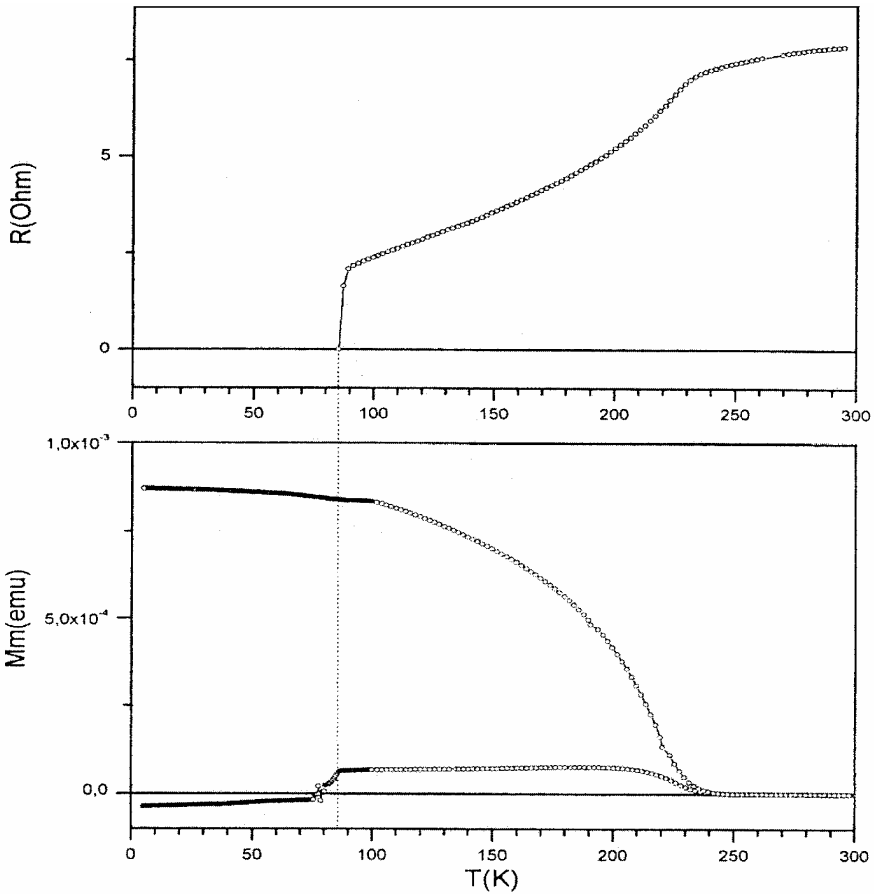

Fig. (8): Resistance (upper panel) and magnetic moment (lower panel) of a (100nm YBCO - 10nm STO- 100 nm LCMO)$_5$ superlattice as a function of temperature.

Acknowledgements:

The authors would like to thank Ch Bernhard and T. Holden for numerous discussions concerning the optical properties of FM/Sc superlattices and the physics involved. They are grateful to G.van Tendeloo and O. I. Lebedev (EMAT – University of Antwerp Belgium) for the expert TEM work. E. Brücher we thank for the SQUID measurements, K. Förderreuther and B. Lemke for the lithography and contact work.

References:

1. *"Superconductivity in Ternary Compounds II*" Topics Current phys. Vol. 34, M.B. Maple and ∅. Fischer, edts. (Springer, Berlin, 1982),
2. M.B. Maple, *Physica C* **341-348**, 47 (2000).
3. L. Bauernfeind, W. Widder, and H.-F Braun, *Physica C* **254**, 151 (1995).
4. C. Bernhard, J. L. Tallon, Ch. Niedermayer, Th. Blasius, A. Golnik, E. Brücher, R. K. Kremer, D. R. Noakes, C. E. Stronach and J. Ansaldo, *Phys. Rev. B* **59**, 14 099 (1999).
5. C. W. Chu, *Physica C* **341-348**, 25 (2000)
6. C. Strunk, C. Sürgers, U. Paschen and H. Von Löhneysen, *Phys. Rev. B* **49**, 4052 (1994).
7. M. Kasai, T. Ohno, Y. Kanke, Y. Kozono, M. Hanazono, Y. Sugita, *Jpn. J.Appl. Phys.* **29**, L 2219 (1990).
8. G. Jakob, V.V. Moschalkov, Y. Bruynseraede, *Appl. Phys. Lett* **66**, 2564 (1995).
9. A.M. Goldman, V. Vas'ko, P.Kraus, K. Nikolaev, and V.A. Larkin *J. of Magn. and Mag. Mat* **200**, 69 (1999).
10. D. Dijkamp and T. Venkatesan, *Appl. Phys. Lett*. **51**, 619 (1987).
11. H.-U. Habermeier, Eur. *J.Solid State Inorg. Chem* **28**, 201 (1991).
12. H.-U. Habermeier and G. Cristiani to be published.
13. E. E. Fullerton, I. K. Schuller, H. Vanderstraten, and Y. Bruynseraede, *Phys. Rev*, *B* **54**, 9292 (1992)
14. R. B. Praus, B. Leibold, G. M. Gross, and H.-U. Habermeier, *Appl. Surf. Sci.* **138-139**, 417 (1999).
15. Th. Schuster, H. Kuhn, E.H. Brandt, M.V. Indenbohm, M. Kläser, G. Müller-vogt, H. –U. Habermeier, H. Kronmüller, and A. Forkl, *Phys. Rev. B* **52**, 10375 (1995).
16. C.W. Chu *Physica C* **341-348**, 25 (2000).
17. H. –U. Habermeier, G. Gristiani, R. K . Kremer, O. Lebedev, and G. Van Tendeloo, *Physica C* **364-365**, 298 (2001).
18. S.-W. Cheong and H.Y. Hwang, in Tokura, Y. (Ed.) *"Contributions to Colossal Magnetoresistance Oxides*", Monographs in Condensed Matter Science, Gordon and Breach, London 1999.
19. C.A.R. Sa de Melo, *Phys. Rev. Lett*. **79**, 1933 (1997).
20. L. Jansen and R. Block, *Physica A* **252**, 278 (1998).
21. Q.Li,X.X.Xi.D.Wu,A. Inam, S. Vladamanati, V. L. McLean, T.Venkatesan, R. Ramesh, D.M. Hwang, J.A Martinez, and L. Nazar, *Phys. Rev. Lett* **64**, 3086 (1990).
22. D.H. Lowndes, D.P. Norton, and J.D. Budai, *Phys. Rev. Lett*. **65**, 1160 (1990)
23. T. Holden, C. Bernhard, F. Greissl, A. Golnik, A. Pimenov, J. Humlicek, B. Keimer, G. Cristiani and H.-U Habermeier, Submitted to *Phys Rev. Lett*. (2002).